



Steroid hormone receptors through *Cry2* are key players in the circadian clock response to serum

Received: 24 April 2025

Accepted: 27 November 2025

Published online: 07 December 2025

Check for updates

Gal Manella ^{1,2,4}, Saar Ezagouri ^{1,4}, Nityanand Bolshette ^{1,4}, Achim Kramer ³, Marina Golik¹, Yaarit Adamovich ¹ & Gad Asher ¹

Circadian clocks are cell-autonomous oscillators that are present in most cells of the body and temporally coordinate their function. Alignment of cellular clocks with each other and the environment is mediated mostly through blood borne signals. Although serum is a potent resetting signal for circadian clocks, the underlying intracellular molecular underpinnings are largely unknown. Here, we employ Circa-SCOPE, a high-throughput single-cell method for constructing Phase Transition Curves (PTCs), to classify intracellular signaling pathways and clock-components that participate in clock resetting by serum. We identify steroid hormone, including sex-hormone receptors as key mediators of serum-induced phase resetting. Unexpectedly, we discover that *Cry2* plays a central role in the response to serum and specifically to steroid hormones, irrespectively of its effect on the clock period-length. Furthermore, we find that PTCs are largely unaffected by the period-length. Overall, our findings provide important insight on intracellular determinant of the clock response to serum.

Circadian clocks are endogenous molecular timekeeping mechanisms with a period length of ~24 h. These clocks temporally coordinate myriad behavioral, physiological and metabolic processes with external daily rhythms^{1–3}. Circadian misalignment is associated with various pathologies, including sleep disorders, metabolic syndromes, cancer, and neurodegenerative diseases⁴.

The molecular circadian clockwork is present in most cells of the body and relies on interlocked negative transcription-translation feedback loops. The basic helix-loop-helix-PER-ARNT-SIM (bHLH-PAS) proteins BMAL1 and CLOCK heterodimerize and drive the expression of the *Period* (i.e., *Per1-3*) and *Cryptochrome* (i.e., *Cry1-2*) genes. Subsequently, PER and CRY proteins accumulate and repress the transcription of their own genes. A second feedback loop includes the orphan nuclear receptors of the REV-ERB and ROR families^{5,6}.

The mammalian circadian timing system is structured in a hierarchical manner and consists of a central pacemaker in the

suprachiasmatic nucleus (SCN) of the brain and peripheral clocks in most cells of the body. The communication between the central and peripheral clocks in the rest of the body is vital for maintaining phase coherence between them. Clocks' alignment throughout the body relies on various time-signals, many of which are blood-borne signals^{7–9}. However, the intracellular signaling pathways and the specific clock components that respond to blood-borne signals and reset the clock are partially known¹⁰.

The extent and direction that a given stimulus shifts the clock is dose- and time-dependent. Therefore, a representation of the phase after the intervention as a function of the phase before the intervention (a.k.a. Phase Transition Curve (PTC)) is necessary to comprehensively depict the resetting effect of the signal¹¹. As PTC experiments are usually low-throughput and labor-intensive, we recently developed Circa-SCOPE, a method for high-throughput PTC reconstruction based on single-cell live microscopy¹². Hitherto, Circa-SCOPE capacity to

¹Department of Biomolecular Sciences, Weizmann Institute of Science, Rehovot, Israel. ²Division of Biology and Biological Engineering, California Institute of Technology, Pasadena, CA, USA. ³Laboratory of Chronobiology, Charité - Universitätsmedizin Berlin, Berlin, Germany. ⁴These authors contributed equally: Gal Manella, Saar Ezagouri, Nityanand Bolshette. e-mail: gad.asher@weizmann.ac.il

generate dozens of high-resolution PTCs simultaneously enabled us to successfully study the clock response to a wide variety of signals either alone or in combination^{12,13}.

As aforementioned, despite the efficient capacity of serum to reset the clock, several aspects remain uncharted. In particular, which intracellular signaling pathways are involved, and through which clock components they act. To address these questions, we employed Circa-SCOPE and examined the effect of inhibitors of various intracellular signaling pathways on the capacity of serum to shift the clock. Our screen provides a quantitative depiction of several known, as well as unknown, signaling pathways and highlights the role of steroid hormone receptors as key mediators of clock resetting by serum. The surge in *Per1* and *Per2* expression in response to serum raised the notion that they are implicated in clock resetting¹⁴. Unexpectedly, our genetic loss-of-function experiments revealed a prominent role for *Cry2* in mediating the clock's response to serum, and specifically to steroid hormones, in cultured cells. We further show that the effect of *Cry2* on clock resetting by serum is independent of its effect on the clock period length, and that PTCs are largely unaffected by differences in period length.

Results

Screening for intracellular signaling pathways that are implicated in clock resetting by serum

We and others previously showed that serum acts as a potent phase-resetting signal^{9,15}. To identify intracellular signaling pathways through which serum resets the clock, we employed Circa-SCOPE and screened for various inhibitors of signaling pathways in response to rat serum (Fig. 1). To this end, we employed NIH3T3 cells expressing a dual reporter system (Nuclear marker: H2B-mCherry, Circadian reporter: *Rev-Erba*-Venus) in conjunction with the circadian single-cell oscillators PTC extraction (Circa-SCOPE) protocol (Fig. 1a, b)¹².

The premise of our pharmacological loss-of-function screen is that any inhibitor that modulates the PTC of rat serum would implicate the associated pathway in serum-induced phase resetting. We tested 25 inhibitors as a background treatment for cells that were subsequently exposed to rat serum. Out of these, 8 inhibitors significantly modulated the serum-induced PTC, shifting it from a type-0 to a type-1 response (Fig. 1c and PTC profiles alongside their characteristics in Supplementary Fig. 1a-c, see also Supplementary Data 1-3). The inhibitors with significant effects on the rat serum PTC were 10058-F4 (c-Myc inhibitor), CH-223191 (aryl hydrocarbon receptor inhibitor), Cyproterone Acetate (Androgen receptor (AR) inhibitor), GSK2982772 (RIPK1 inhibitor), KN-93 Phosphate (Calmodulin-dependent protein kinase II inhibitor), VO-Opfic trihydrate (PTEN inhibitor), CCG-1423 (Rho/MK1/SRF inhibitor), and Pictilisib (PI3K α/δ inhibitor).

Interestingly, in addition to the AR inhibitor, two other steroid hormone receptors, the glucocorticoid and progesterone receptors (GR and PR, respectively), were previously implicated in clock resetting as their activation through dexamethasone and progesterone, respectively, elicits a phase response within the nanomolar range¹².

Our previous work uncovered an intricate interaction between different phase-resetting signals¹³. Given the likelihood that serum consists of a variety of resetting signals, we hypothesized that the effect of less potent resetting signals, might be masked by the presence of more potent resetting signals such as corticosterone and potentially progesterone¹³. We, therefore, conducted a second screen in the presence of Mifepristone (MF) as a background treatment. MF is a potent anti PR, and to a much lesser extent anti GR and AR¹⁶. Because MF blunts the phase resetting effect of rat serum¹², we applied a higher dose of rat serum to obtain a significant PRC and to raise the levels of potentially less effective compounds (Fig. 1d and PTC profiles alongside their characteristics in Supplementary Fig. 1d, e). Out of the 25 inhibitors tested in combination with MF, 5 modified the PTC of rat serum. The treatments varied in their pattern of response and were

grouped as follows: the first group includes inhibitors that rendered the PTC of rat serum and MF non-significant, namely, blunted the response, such as Brilanestrant (Estrogen receptor (ER) inhibitor), and Dorsomorphin (AMPK inhibitor) (Fig. 1d and Supplementary Fig. 1d, e). The second group consists of inhibitors that enhanced phase resetting by modifying the PTC of MF and rat serum from type 1 to type-0, thus antagonizing MF's effect on rat serum-induced PTC. This group includes Bosutinib (Src inhibitor), CCG-1423 (Rho/MK1/SRF inhibitor), and Pictilisib (PI3K α/δ inhibitor) (Fig. 1d; Supplementary Fig. 1d, e). Interestingly, when administered with rat serum alone, the inhibitors Pictilisib and CCG-1423 attenuated the PTC of rat serum, whereas when added in combination with MF, they potentiated the PTC of rat serum (Fig. 1c, d). This suggests that these drugs antagonize MF's effect on the rat serum-induced phase response.

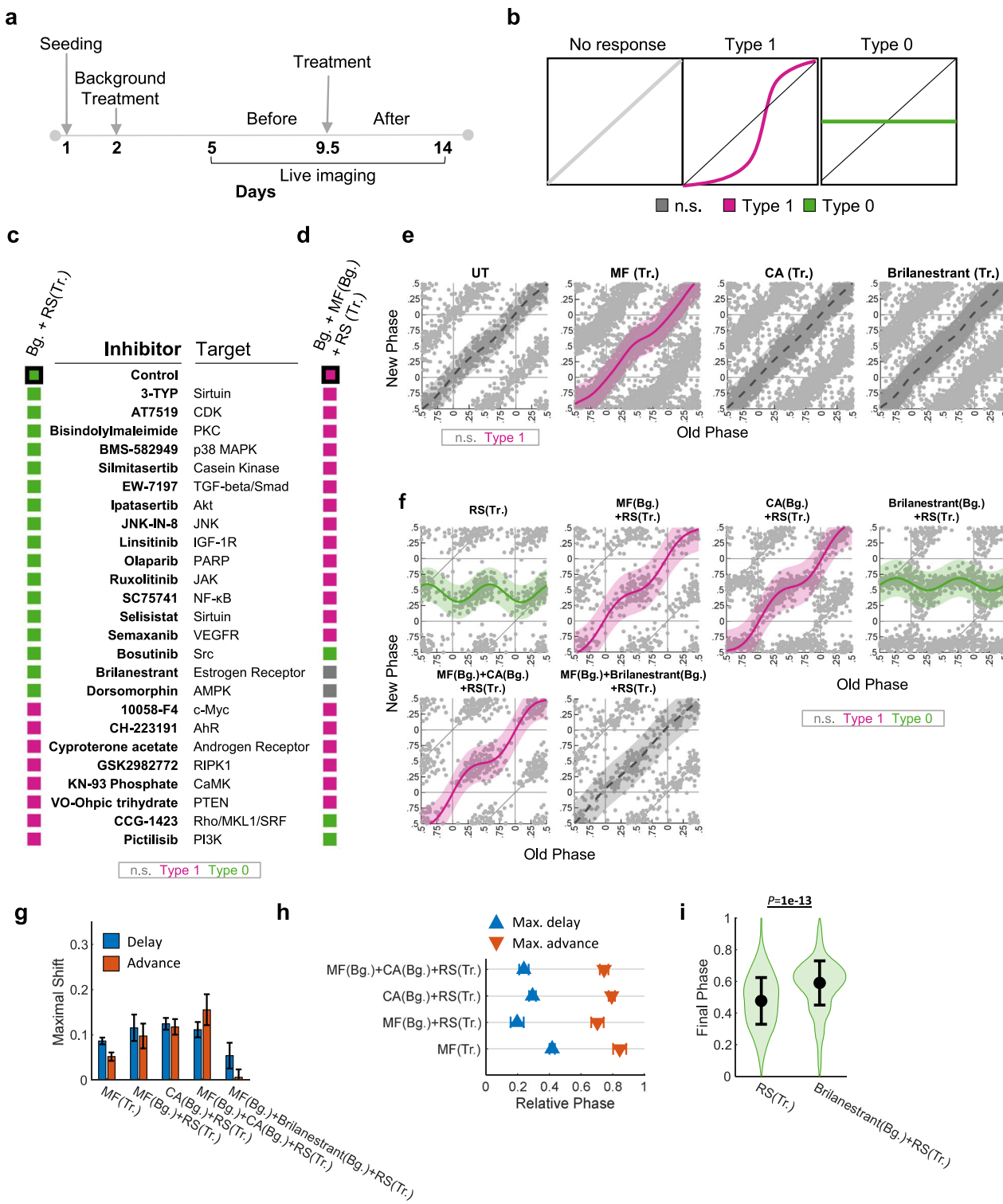
In line with our previous report, MF as a treatment elicited type-1 PTC (Fig. 1e, g, h)¹². By contrast, the AR or the ER inhibitors (Cyproterone Acetate (CA) and Brilanestrant, respectively) did not elicit a significant effect as a treatment alone (Fig. 1e). When the steroid hormone receptor inhibitors MF or CA were applied as background to rat serum treatment, they shifted the effect of serum from type-0 to type-1 (Fig. 1f-h). By contrast, the ER inhibitor (Brilanestrant) had only a mild effect on the final phase (Fig. 1f, i). Importantly, triple inhibition of GR and PR (MF) together with ER (Brilanestrant) completely inhibited serum-induced phase resetting (Fig. 1f), suggesting that together these steroid hormone receptors cover the lion's share of the clock response to serum.

Taken together, our inhibitor screens identified several compounds (11 of the 25 inhibitors tested) that modulate serum-induced PTC either alone or in combination with MF. Importantly, two of these inhibitors, Brilanestrant and CA, target steroid hormone receptors (ER and AR, respectively), and together with MF (PR and GR inhibitors) highlight the key role of steroid hormone receptors in clock resetting by serum.

The cross talk between different steroid hormones in serum-induced phase resetting

Hitherto, our pharmacological screen identified steroid hormone receptors (GR, PR, ER and AR) as key mediators of serum-induced phase resetting (Fig. 1 and Supplementary Fig. 1). Steroid hormones are broadly grouped to corticosteroids (glucocorticoids and mineralocorticoids) and sex hormones (progesterone, androgens, and estrogens). These lipophilic small molecules bind to their respective intracellular receptors (e.g., GR, PR, ER, and AR) in the cytoplasm and shuttle them to the nucleus to transcriptionally regulate a myriad of cellular functions. To examine whether these steroid hormones reset the clock through converged or diverged pathways, we set out to test their interactions in phase resetting.

Previously, we showed that background levels of a resetting signal (e.g., dexamethasone or forskolin) attenuate the effect of a subsequent dose of the same signal, and this effect depends on the reactivation of the same signaling pathway¹³. For example, background dexamethasone treatment attenuated the response to dexamethasone or corticosterone, consistent with the fact that they both function through GR activation, but not of forskolin and vice versa¹³. Similarly, background treatment with progesterone inhibited the response to progesterone treatment (Supplementary Fig. 2a, b and Supplementary Data 5) in a dose-dependent manner. Next, we examined the effect of background progesterone-treatment on the phase response to dexamethasone and found that progesterone inhibited the phase response of the clock to dexamethasone as well in a dose-dependent manner (Fig. 2a, b and Supplementary Data 4). Thus, despite acting through different nuclear receptors, progesterone inhibited clock resetting by dexamethasone. We cannot exclude the possibility that the observed effect may reflect receptor desensitization or nonspecific cross-pathway interference. Alternatively, it may hint that these two



molecules function through a common nominator, potentially within the core clockwork.

Cry2 plays a role in serum-induced phase resetting

We and others previously showed that different resetting signals induce an immediate response in the expression of several core clock genes^{12,14,17}. Similar to SCN of animals receiving a light pulse¹⁸, a rapid surge in expression of the clock genes *Per1* and *Per2* was observed in response to serum⁷. This association raised the possibility that *Per*'s are implicated in the signaling cascade that elicits the phase shift of the clock in response to serum. However, hitherto their role was never

functionally tested. We, therefore, set out to test the function of *Per*'s and other clock components in response to serum. To this end, we performed genetic loss of function experiments by knocking down different core clock genes using siRNAs and analyzing the PTC in response to serum (Fig. 3a). We hypothesized that if knockdown of a core clock component alters the PTC in response to serum, it would indicate that this component plays a role in conveying the resetting signal to the oscillator eliciting a phase shift. For obvious reasons, this approach cannot be applied with the essential clock components of the positive arm of the feedback loop, which, in their absence, rhythmicity is lost in cultured cells (i.e., *Bmal1* and *Clock* in cultured cells¹⁹).

Fig. 1 | Screening for intracellular signaling pathways that are implicated in clock resetting by serum. **a** Schematic representation of the experimental design. Briefly, one day following seeding, the culture media was replaced, and background treatment was administered as applicable. Subsequently, cells were allowed to desynchronize for three consecutive days. Next, cells were imaged continuously for a total of 9 days. Midway through the recording period (day 9.5), a treatment (e.g., rat serum) was applied to the cells. Images were collected and single-cell rhythmicity was assessed before and after the perturbation. Subsequently, the data were used to construct phase transition curves (PTCs). **b** Schematic representation of PTC types. Non-significant, Type 1 and 0 PTCs are colored in gray, purple and green, respectively, throughout the paper. **c, d** Heatmap representation of the results of the inhibitor screen for intracellular signaling pathways. **c** Cells were treated with various inhibitors of intracellular signaling pathways as background to rat serum (RS) treatment (0.4%), or **d** as background together with Mifepristone (MF, 1.25 μ M) to RS (2%) treatment. The heatmaps summarize the classification of PTCs: non-significant (gray), type-1 (purple) and type-0 (green), with each condition compared to its corresponding control group, vertically. Inhibitors were supplemented at 100 nM concentration in all cases. (see “Methods” for details on statistical testing of phase responses; exact P values for response and type-0 can be found in the Source Data file) **e** PTCs of untreated (UT) control population, or Mifepristone (MF), Cyproterone Acetate (CA), and Brilanestrant provided as treatment (Tr.) with no background (Bg.), ($n = 341, 1402, 1185, 1533$ cells respectively). Throughout the

study, each point represents the phases of a single cell. Data are double-plotted for clarity. Throughout the study, phases are normalized to the corresponding period length (relative phase units between [0, 1]). Shown as type 1 resetting model curve \pm 95% confidence interval, Pink: significant resetting, gray: nonsignificant ($P > 0.05$) in bootstrapping test for response (exact P values for response and type-0 can be found in the Source Data). **f** PTCs of RS-treated (Tr.) cells with either no background (Bg.), or background of MF, CA, Brilanestrant, MF + CA, MF + Brilanestrant, or MF+ Brilanestrant+ RS. ($n = 196, 143, 301, 348, 155$, and 159 cells respectively, pink: type 1 resetting model \pm 95% confidence interval, green: type 0 resetting model \pm 95% confidence interval, gray: nonsignificant ($P > 0.05$) in bootstrapping test for response; exact P values for response and type-0 can be found in the Source Data file). **g** Maximal phase delay (Delay) and advance (Advance) and **h** the phase of maximal phase delay and advance, calculated from the type 1 PTCs for MF as treatment, or RS-treated with MF in background (MF + RS), CA in background (CA + RS) or both (MF + CA + RS), shown in **(e, f)**. Also included the MF(Bg.)+Brilanestrant(Bg.)+RS(Tr.) condition, which showed no significant phase response, for the sake of presentation. Shown as value \pm SD, the standard deviation is estimated from bootstrapping. **i** The final phase distributions of the presented Type 0 PTCs, namely rat serum (RS) without or with Brilanestrant as background (shown in **(f)**). ($n = 196, 348$ cells, circular mean \pm SD, two-sample Watson–Williams test, $P < 0.05$ in bold). See also Supplementary Data 1–3.

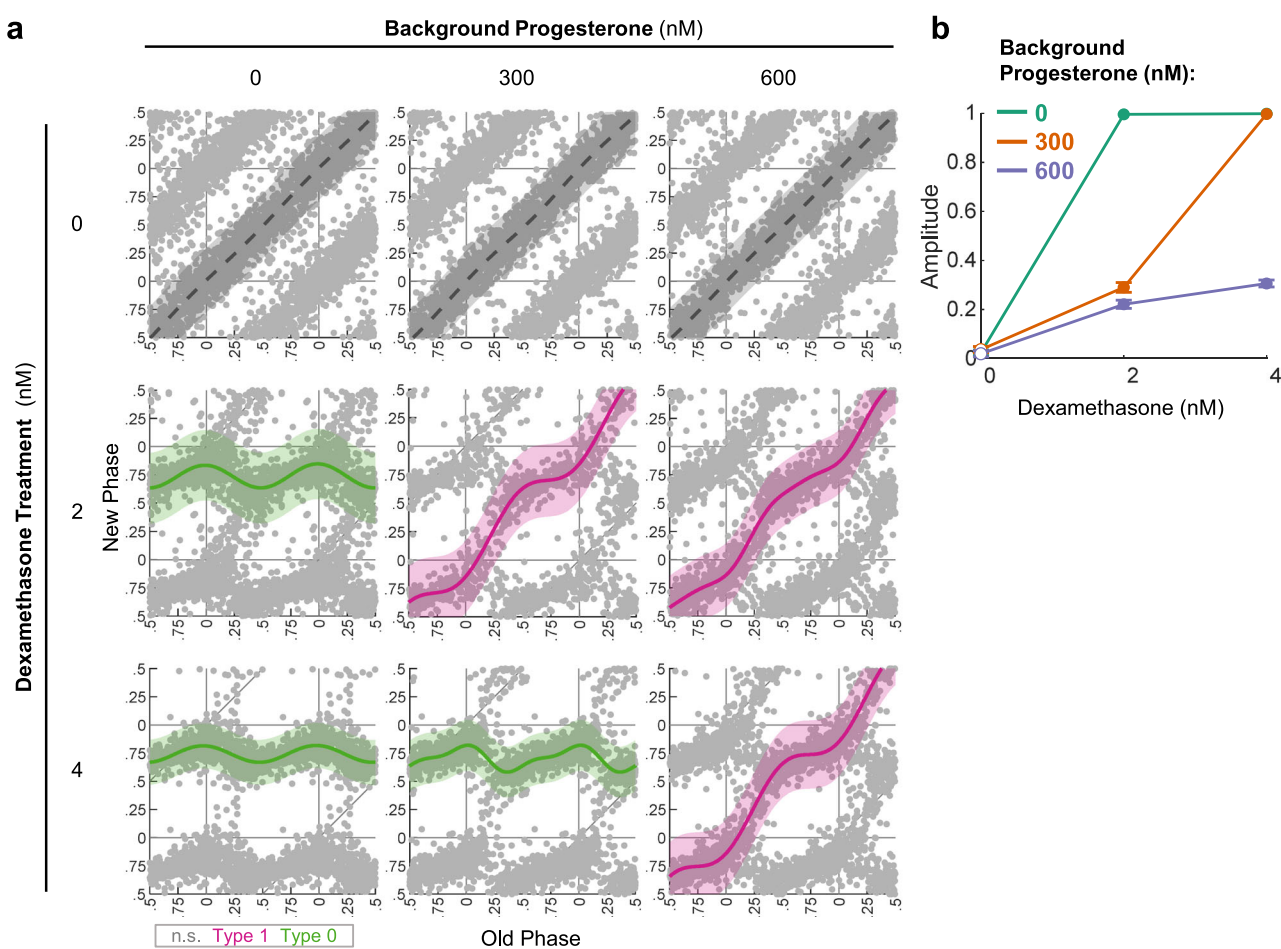


Fig. 2 | The interaction between dexamethasone and progesterone in phase resetting. **a** Increasing doses of progesterone were added in background media, and then cells were treated with increasing doses of dexamethasone. Depicted are the PTCs reconstructed from each background-treatment combination. (Dex 0 nM $n = 1031, 885, 708$; Dex 2 nM $n = 869, 414, 770$; Dex 4 nM $n = 868, 729, 663$ cells; Pink: type 1 resetting model \pm 95% confidence interval, green: type 0 resetting model \pm 95% confidence interval, gray: nonsignificant ($P > 0.05$) in bootstrapping

test for response; exact P values for response and type-0 can be found in the Source Data file). **b** The PTC amplitude (i.e., the absolute difference between maximal delay and maximal advance) of the different combinations. Value \pm SD as estimated from bootstrapping, note that type-0 has maximal amplitude by definition, thus no error bars are shown. (sample sizes the same as in **(a)**; Full marks, $P < 0.05$ in bootstrapping test for response as in **(a)**; empty marks, $P > 0.05$). See also Supplementary Data 4.

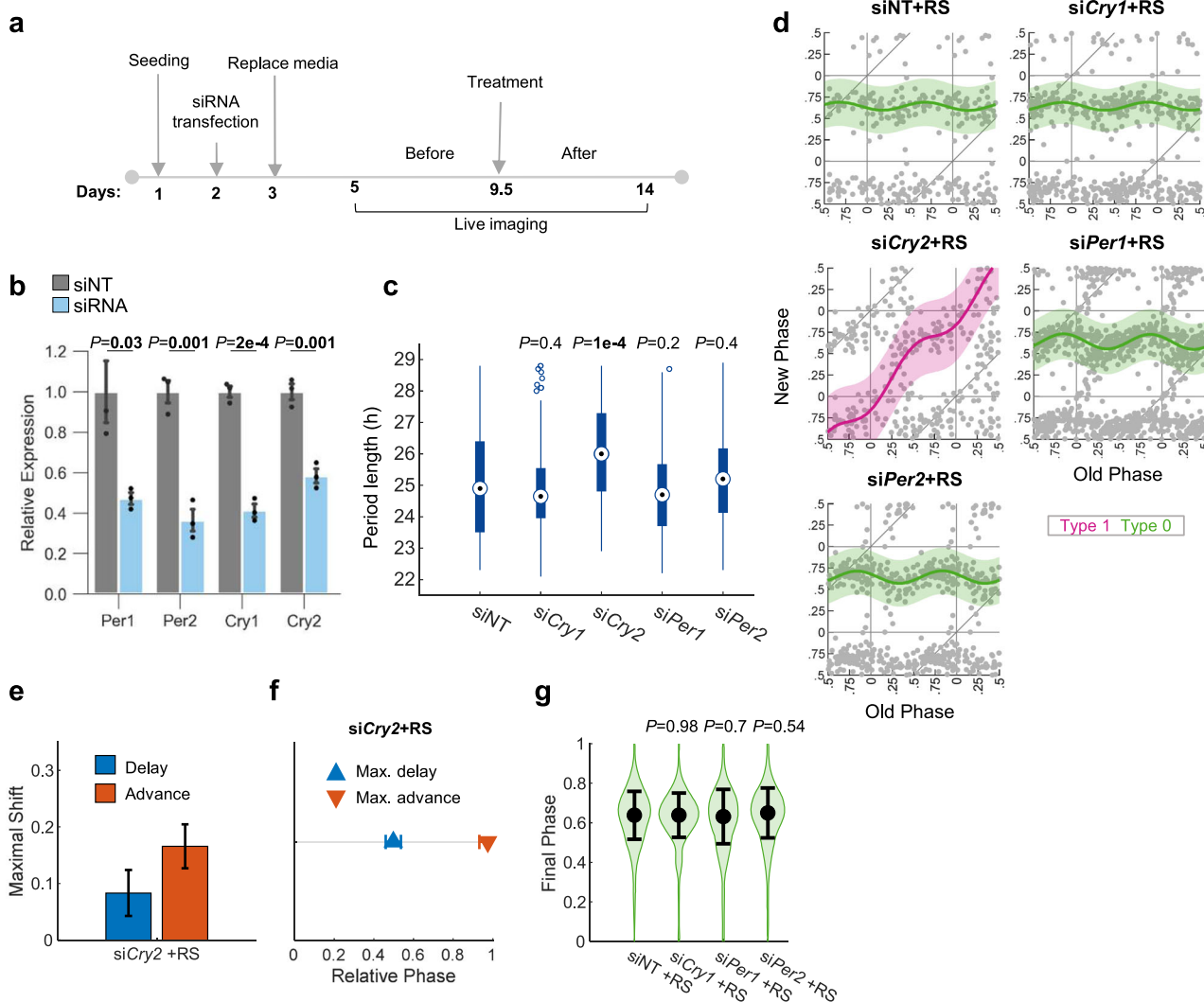


Fig. 3 | Cry2 modulates serum-induced phase resetting. a Schematic representation of the experimental design. Cells were transfected with siRNA treatment on the second day; media was replaced on the third day. **b** The relative expression of different clock genes between siNT (Non-Targeting control) and the specific siRNA for each of the indicated clock genes as determined by quantitative real-time PCR. (Mean \pm SD; $n = 3$ biological replicates per condition; two-sample two-sided Student's t test compared to siNT, $P < 0.05$ in bold). **c** Period differences between siNT and the specific siRNA for each of the indicated clock genes as determined by Circa-SCOPE before treatment ($n = 73, 100, 106, 139$, and 187 cells, respectively; two-sample two-sided Student's t test compared to siNT, $P < 0.05$ in bold; central circle: median; box: interquartile range (IQR); whiskers: extend to the maximal/minimal values within the range of ± 1.5 IQR; circles: outliers). **d** PTC profiles for siNT and the specific siRNA for each of the indicated clock genes as determined by Circa-

SCOPE upon treatment with rat serum (RS, 2%). ($n = 79, 128, 86, 274$, and 139 cells, respectively). Pink: type 1 resetting model $\pm 95\%$ confidence interval, green: type 0 resetting model $\pm 95\%$ confidence interval, gray: nonsignificant ($P > 0.05$) in bootstrapping test for response; exact P values for response and type-0 can be found in the Source Data file). **e** Maximal phase delay (Delay) and advance (Advance) calculated from the presented type 1 PTCs for siCry2 with rat serum. Shown as value \pm SD as estimated from bootstrapping. **f** The phase of the maximal phase delay (Delay) or advance (Advance) calculated from the presented type 1 PTC for siCry2 with rat serum. Shown as value \pm SD as estimated from bootstrapping. **g** The final phase distributions of the presented Type-0 PTCs in **d**. ($n = 79, 128, 274$, and 139 cells, respectively; circular mean \pm SD, two-sample Watson–Williams test compared to the siNT + RS). See also Supplementary Data 6.

We, therefore, focused on the negative arm, and successfully knocked down *Per1*, *Per2*, *Cry1*, and *Cry2* (Fig. 3b). In line with previous analyses in cultured cells, knocking down of *Cry2* lengthened the period-length (Fig. 3c)¹⁹. Using Circa-SCOPE, we constructed the serum-induced PTC in the presence of control non-targeting siRNA (siNT) or the different specific clock component siRNAs. As expected, serum induced a Type-0 PTC when treated with siNT (Fig. 3d). By contrast, the PTC of serum was exclusively altered by *Cry2* knockdown, shifting it from Type-0 to Type-1 (Fig. 3d–f and Supplementary Data 6). Knockdown of the other targets did not elicit a significant effect (Fig. 3g). We examined the effect of *Cry2* knockdown on *Per1* or *Per2* mRNA expression levels in response to serum stimulation and found no significant effect on either *Per1* or *Per2* induction (Supplementary Fig. 3). This suggests that

the effect is likely independent on the *Per1* or *Per2* transcript levels and is consistent with our observation that knockdown of these genes does not alter the PTC of serum (Fig. 3d). Notably, *Cry2* transcript levels do not exhibit any immediate response to serum, and its knockdown did not elicit major effects on the transcriptional response of clock genes to serum stimulation (Supplementary Fig. 3a, b). This may hint towards the potential involvement of post-transcriptional mechanisms in the role of *Cry2* in clock resetting by serum.

As noted above, knockdown of *Cry2* results in a longer mean period-length among the population, unlike the other siRNA treatments. It is possible that the effect on the phase response is due to the shifted period distribution, and not specifically due to *Cry2* deficiency. To exclude this hypothesis, we performed a resampling analysis, where

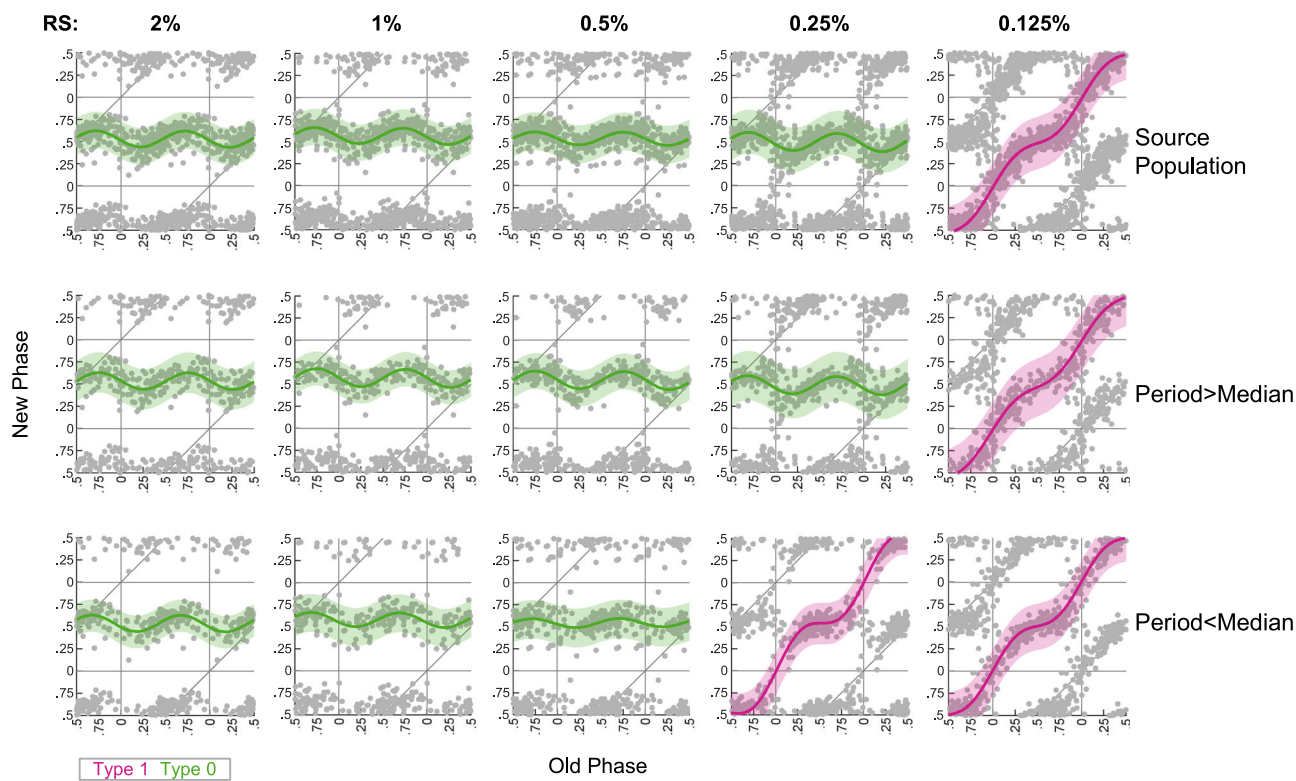


Fig. 4 | The effect of period length on the phase response. Data reanalyzed from ref. 12. PTCs were reconstructed for different doses of rat serum (RS). The source population (first row) of each dose was divided into two equal subpopulations: one with periods above the median (second row), and the second one with periods below the median (third row). Medians were calculated per dose (source

populations $n=278, 250, 303, 403$, and 398 ; Pink: type 1 resetting model $\pm 95\%$ confidence interval, green: type 0 resetting model $\pm 95\%$ confidence interval; gray: nonsignificant ($P > 0.05$) in bootstrapping test for response; exact P values for response and type-0 can be found in the Source Data file). See also Supplementary Data 8.

the siNT population was resampled according to the period distribution in the *siCry2* population. The resampled population shows a type-0 response, comparable with the response in the source population. Thus, indicating that the period distribution is not sufficient to explain the phase response attenuation upon *Cry2* knockdown (Supplementary Fig. 4a–c and Supplementary Data 7). The reciprocal analysis, namely sampling from the *siCry2* population to match the siNT distribution, exhibits type-0 response (Supplementary Fig. 4d–f). It is expected that *siCry2* effect on both the period and the phase response will correlate, and hence short-period cells are also least affected in terms of PTC strength. Finally, as oscillation amplitude can also affect resetting strength²⁰, we also tested whether there are any differences in amplitude or initial synchrony between *Cry2* knockdown and control and found no significant effects (Supplementary Fig. 5a, b). This suggests that the observed effect of *Cry2* on clock resetting is independent of amplitude or initial phase distribution.

We further corroborated our findings on the effect of *Cry2* knockdown on serum-induced clock resetting using the serum mimetic, B-27, an optimized serum-free supplement. Here again, the results showed that knockdown of *Cry2* alters the PTC, shifting it from Type-0 to Type-1 (Supplementary Fig. 6a), alongside a longer circadian period (Supplementary Fig. 6b).

Collectively, our results with serum and serum mimetic suggest that *Cry2* plays a role in serum-induced phase resetting, irrespective of its effect on the clock period length.

The phase response is largely unaffected by the clock period length

The effect of *Cry2* on serum-induced phase-response (Fig. 3d, e and Supplementary Fig. 4) was independent of the circadian period. This

prompted us to further explore the potential relationship between the clock period length and the phase response. To this aim, we reanalyzed Circa-SCOPE PTC data for a dose-dependent response to rat serum ranging from type 1 to 0. The PTCs were reconstructed for cells with period length below or above the median period length of the entire population. Our analysis shows that overall, the PTC type remained largely similar between the two groups and the entire population, apart from the case of 0.25% rat serum with a period shorter than the median (Fig. 4 and Supplementary Data 8). Similarly, we could not observe major effects of oscillation amplitude on the PTC (Supplementary Fig. 5c).

We, therefore, concluded that the period length does not largely influence the PTC type, further supporting that the effect of *Cry2* on serum-induced PTC is independent of its effect on the circadian period.

Cry2 regulates phase resetting induced by distinct intracellular signaling pathways

Our findings that *Cry2* regulates the clock response to serum and serum mimetic raised the question whether the regulation of phase resetting by *Cry2* is pathway-specific or general. To address this, we examined different resetting signals: dexamethasone, progesterone and forskolin. These potent phase-resetting signals activate distinct signaling pathways, namely, GR, PR, and Adenylate Cyclase, respectively. These signaling pathways were also reported to be activated by serum^{21,22}. It is noteworthy that among sex hormones, unlike progesterone, which acts as a potent phase-resetting signal, estradiol does not elicit a significant phase response¹².

PTCs were constructed for each compound added as a treatment to cells pre-treated with *siCry2* or *siNT* as a control (Supplementary

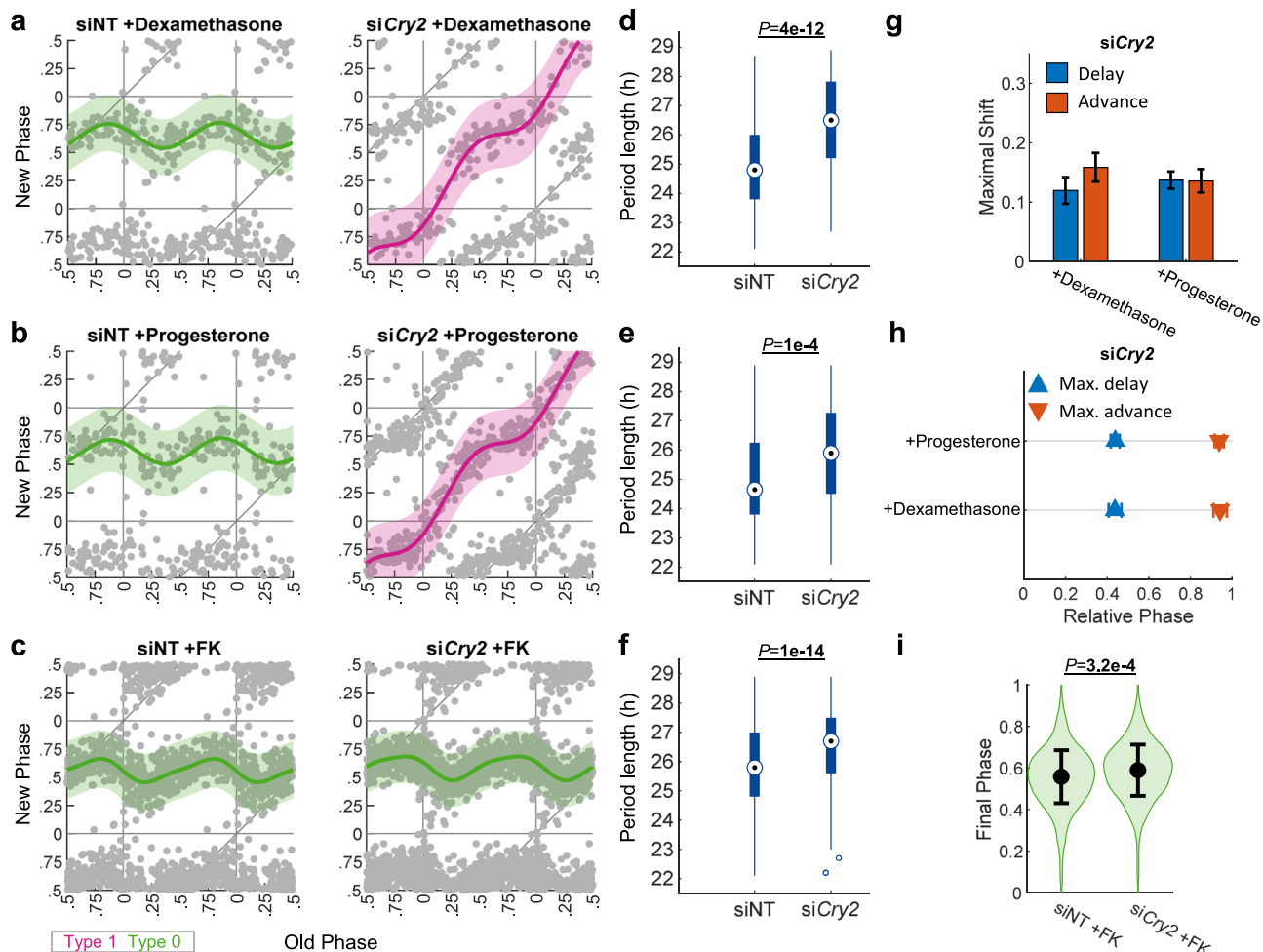


Fig. 5 | Cry2 regulates phase resetting induced by distinct intracellular signaling pathways. Cells were treated with control (siNT) or siCry2 and subsequently exposed to (a) 4 nM dexamethasone ($n = 119, 101$ cells), (b) 600 nM progesterone ($n = 100, 183$ cells), and (c) 4 μ M FK treatments ($n = 420, 611$ cells), and PTCs were constructed. pink: type 1 resetting model $\pm 95\%$ confidence interval, green: type 0 resetting model $\pm 95\%$ confidence interval, gray: nonsignificant ($P > 0.05$) in bootstrapping test for response; exact P values for response and type-0 can be found in the Source Data file. Period distributions before (d) dexamethasone ($n = 119, 101$ cells), (e) progesterone ($n = 100, 183$ cells), and (f) FK treatments ($n = 420, 611$ cells), corresponding to the PTCs in (a–c). Two-sample two-sided Student's t test was $P < 0.05$ in bold. Central circle: median; box: interquartile range (IQR); whiskers: extend to the maximal/minimal values within the range of ± 1.5 IQR; circles: outliers. (g) Maximal phase delay (Delay) and advance (Advance) calculated from the presented type 1 PTCs for siCry2 with dexamethasone and progesterone in (a, b). Shown as value \pm SD as estimated from bootstrapping. (h) The phase of the maximal phase delay (Delay) or advance (Advance) calculated from the presented type 1 PTC for siCry2 with dexamethasone and progesterone in (a, b). Shown as Mean \pm SD from bootstrapping. (i) The final phase distributions of the presented Type 0 PTCs in (c) for siNT and siCry2 with forskolin. ($n = 420, 611$ cells, circular mean \pm SD, two-sample Watson–Williams test, $P < 0.05$ in bold). See also Supplementary Data 9.

whiskers: extend to the maximal/minimal values within the range of ± 1.5 IQR; circles: outliers. (g) Maximal phase delay (Delay) and advance (Advance) calculated from the presented type 1 PTCs for siCry2 with dexamethasone and progesterone in (a, b). Shown as value \pm SD as estimated from bootstrapping. (h) The phase of the maximal phase delay (Delay) or advance (Advance) calculated from the presented type 1 PTC for siCry2 with dexamethasone and progesterone in (a, b). Shown as Mean \pm SD from bootstrapping. (i) The final phase distributions of the presented Type 0 PTCs in (c) for siNT and siCry2 with forskolin. ($n = 420, 611$ cells, circular mean \pm SD, two-sample Watson–Williams test, $P < 0.05$ in bold). See also Supplementary Data 9.

Fig. 6c). Remarkably, Cry2 significantly modulated the types of PTCs of dexamethasone and progesterone, but not of forskolin (Fig. 5a–c, g, h, and Supplementary Data 9). As expected, knockdown of Cry2 lengthens the circadian period (Fig. 5d–f). In the case of forskolin, we observed only a minor effect on the final phase (Fig. 5i).

Lastly, to examine the cell type specificity of Cry2 in clock resetting, we employed wild type (WT) and Cry2 knockout (KO) *Bmal1*-luciferase reporter human osteosarcoma cells (U2OS cells)²³. Since to date Circa-SCOPE is optimized to work only with NIH3T3 cells, we performed a simplified assay using a single timepoint treatment with increasing doses of dexamethasone. We observed that Cry2 KO cells reach their maximal phase shift with a higher dexamethasone dose compared to WT cells (Supplementary Fig. 7), suggesting that Cry2 modulates the dose of type-0 transition in U2OS cells.

We concluded that Cry2 participates in phase resetting induced by distinct intracellular signaling pathways such as steroid hormones, rather than a general modulator of the phase response.

CRY2 binds GR and modulates its transcriptional activity

To obtain mechanistic insight on the role of Cry2 in clock resetting, we first examined whether CRY2 physically interacts with GR. We performed co-immunoprecipitation experiments and found, in line with a previous report²⁴, that CRY2 interacts with GR and that this interaction increases upon dexamethasone treatment (Supplementary Fig. 8a). Next, we employed a GRE-luciferase reporter to examine the effect of Cry2 on its activation by dexamethasone using loss-of-function experiments. Notably, we found that in NIH3T3, knockdown of Cry2 reduces the activation of GRE-luciferase reporter (Supplementary Fig. 8b), suggesting that in these cells CRY2 acts as an activator of glucocorticoid signaling (Supplementary Fig. 8b).

Together, our findings raise the possibility that CRY2 participates in clock resetting by serum through physical interaction and modulation of GR activity.

Discussion

Circadian clock misalignment between and within the organism and the environment is associated with various pathologies²⁵. In vivo, cells and tissues are exposed to blood-borne signals that can convey phase resetting signals and likely enforce internal clock alignment. In this study, we employed Circa-SCOPE to screen for the effect of different inhibitors of key intracellular pathways on serum-induced phase resetting. As we were concerned that cotreatment of the different inhibitors with serum might not provide sufficient time for the inhibitors to adequately inhibit the relevant pathway, we pretreated the cells with the inhibitor prior to the serum stimulation. The 3-day pre-treatment was selected mainly for technical reasons, primarily to minimize interventions close to the serum stimulation, which might affect the phase representation at the time of serum administration—a prerequisite for Circa-SCOPE methodology. We, therefore, cannot exclude that some of the negative hits are due to drug turnover or pathway adaptation.

Our screen identified a major role for steroid hormone receptors, including the glucocorticoid, progesterone, androgen and estrogen receptors, in serum-induced phase resetting (Fig. 1 and Supplementary Fig. 1). Triple inhibition of glucocorticoid, progesterone, and estrogen receptors completely abolished the response to serum, suggesting that these steroid hormone receptors cover the lion's share of the clock response to serum-induced phase resetting. Yet it does not exclude the presence of additional, less potent blood-borne time-signals. Indeed, our screen uncovered several other pathways that might be implicated in the clock response to serum. For example, we found that c-Myc inhibition modulates the clock response to serum; this is in line with previous reports supporting a complex interplay between the molecular oscillator and c-Myc, primarily, in cancer cells²⁶. Similarly, the effect of aryl hydrocarbon receptor inhibition aligns with previous works on the regulation of phase and amplitude of clock gene expression by this receptor²⁷. Likewise, the effect of Calmodulin-dependent protein kinase II inhibitor is reminiscent of its role in clock synchronization in SCN neurons²⁸. Finally, the effects of Rho/MKL1/ SRF inhibitor corroborate previous work on the function of SRF as a blood-borne circadian signal⁹.

By contrast, while PTEN was reported to regulate BMAL1 accumulation and activation²⁹, hitherto, there is no evidence that supports its involvement in clock resetting. Furthermore, our literature survey did not find evidence that points toward the involvement of RIPK1 and PI3K α /δ in circadian clocks in general and specifically in clock resetting. Hence, these findings merit further investigation and support the possibility that these signaling pathways are implicated in clock resetting. Notably, androgens have been implicated in the control of circadian behavior, likely through their action on the SCN clock³⁰, yet less is known on their resetting effect on peripheral clocks, as identified herein.

Our second-tier screen was performed with serum, and MF unraveled another set of time-signals, which were likely masked by the dominance of glucocorticoid and progesterone. Interestingly, under these conditions, inhibition of several signaling pathways (i.e., Src, PI3K α /δ and Rho/MKL1/SRF) reverted the phase response from type 1 to 0. This finding highlights an intricate interaction between different resetting signals and points towards the presence of intracellular mechanisms that buffer the clock response, possibly to avoid unwarranted phase shifts. In addition, our second-tier screen identified signaling pathways that their inhibition, in conjunction with serum and MF, completely blunted the response, such as AMPK, which was previously implicated in the clockwork³¹. Last but not least, ER inhibition further adds to the role of steroid hormones and specifically sex hormones in phase resetting.

In summary, our screen corroborated and characterized in depth the phase response to several known signaling pathways and shed light on the potential involvement of additional pathways that hitherto were

not implicated in clock resetting. Furthermore, it demonstrated a potential hierarchy among blood-borne time-signals whereby potent resetting signals mask the presence of other weak signals. It is tempting to speculate that some of these weak signals might act in a cell and tissue-specific manner or emerge under various pathological conditions. Along this line, we previously reported that hypoxia, as well as intermittent hypoxia as occurs in Obstructive Sleep Apnea, shifts the clock in a time- and tissue-specific manner and consequently elicits inter-tissue circadian clock misalignment³².

Next, we investigated which clock component drives or modulates the shift of the clock by serum and serum-associated signals. To this aim, we knocked down different clock components and generated PTCs in response to rat serum, serum mimetic, as well as to specific compounds that activate distinct signaling pathways, such as dexamethasone, progesterone, and forskolin. Previous reports pointed towards *Per1* and *Per2*, as akin to SCN of animals receiving a light pulse¹⁸, their expression was induced in response to serum⁷. Unexpectedly, we identified *Cry2* as a key mediator of phase resetting induced by all these signals except for forskolin. These results suggest that *Cry2* plays a role in transmitting blood-borne phase-resetting signals to the oscillator in a signal-specific manner. Notably, cryptochromes (both CRY1 and CRY2) were reported to interact with the glucocorticoid receptor in a ligand-dependent fashion to repress its transcriptional activity²⁴.

It is noteworthy that the clock response to corticosteroids differs from the response to forskolin in several aspects. We previously showed that background dexamethasone does not affect resetting by forskolin and vice versa¹³. Furthermore, a fold change detection mechanism in clock resetting is present with dexamethasone but not with forskolin¹³. Here we show that the phase response to steroid hormones, including dexamethasone and serum, but not to forskolin, is modulated by *Cry2*. Collectively, these findings suggest that the response to corticosteroids and most likely serum is distinct from the response to forskolin, ranging from the intracellular signaling pathways involved to the entry to the core clockwork.

The study was mainly performed in NIH3T3 fibroblasts using Circa-SCOPE. We also provide additional evidence that our findings are relevant to U2OS cells. Nevertheless, a comprehensive dose-dependent PTC is required to consolidate these findings. Hitherto, establishing Circa-SCOPE in other cell types, such as U2OS, has proven challenging due to various technical hurdles. We were, therefore, unable to characterize the full PTC of U2OS cells in the presence or absence of *Cry2*. Future studies with high-resolution PTC methodologies that are compatible with various cell types are necessary for a comprehensive analysis of phase resetting across different cells. Moreover, as our study is limited to cultured cells, follow-up studies using animal models are needed to assess the *in vivo* relevance of our findings.

Corticosteroids have been widely implicated in circadian clock resetting and are frequently used to synchronize clocks in cultured cells (e.g., dexamethasone). Recently, we showed that sex hormones such as progesterone are potent resetting agents¹². However, a comprehensive characterization of the interaction between corticosterone and sex hormones in clock resetting remained uncharted. Our finding that triple inhibition of glucocorticoid, progesterone, and estrogen receptors completely abolished clock resetting by serum not only highlights their major role as blood-borne resetting signals but also suggests an intricate interaction between them, especially since their levels change throughout the day³³. Moreover, sex hormone levels differ between males and females and are altered with age, throughout the female menstrual cycle, upon pregnancy, various disease states and hormone administration (e.g., birth control pills) and other medications³⁴. These conditions are often associated with circadian clock disruption; hence, it is tempting to speculate that these effects are to some extent related to the interaction between different steroid

hormones and clock resetting. It will be interesting to examine how sex hormones interact with other clock-modulating signals to reset the clock using Circa-SCOPE alongside other powerful modalities such as modeling phase resetting using singularity response parameters^{35,36}. Furthermore, it will be informative to further experimentally examine the potential connection between the period, amplitude and the phase response³⁷.

In summary, our study characterized intracellular signaling pathways and clock components that participate in clock resetting by serum. Steroid hormone receptors emerge as key mediators of serum-induced phase-resetting. Furthermore, *Cry2* appears as a central regulator of the response to serum, particularly to steroid hormones, independently of its effect on the circadian period. Overall, our findings provide important insight into the intracellular determinants of the clock response to serum.

Methods

Circadian single-cell oscillators PTC extraction (Circa-SCOPE)

For the construction of PTCs, we used the Circa-SCOPE method as previously described¹². In short, NIH3T3 cells expressing a dual reporter system (Nuclear marker: H2B-mCherry, Circadian reporter: *Rev-Erba*-Venus) were seeded in 24-well plates and media was replaced the next day with FluoroBrite Dulbecco's modified Eagle's medium (DMEM) (Gibco) supplemented with 1% fetal bovine serum (FBS) (Gibco), 1 mM glutamine (Biological Industries), 100 U/mL penicillin, and 100 mg/mL streptomycin (Biological Industries). Cells were incubated for 3 additional days and then placed in the IncuCyte (Sertorius) incubated microscope and imaged for 9 consecutive days at 1-h intervals in red and green fluorescence channels as well as phase contrast. Background treatment was introduced at day 2 post-seeding and treatment at day 9.5 post-seeding (see scheme in Fig. 1a). Upon imaging completion, images were extracted and analyzed using our computational pipeline¹²: A CellProfiler (version 3.1.9, Broad Institute³⁸) pipeline was used for illumination correction, nuclei segmentation, tracking, and fluorescence quantifications. Subsequent analyses on the output were conducted with MATLAB (R2020b, MathWorks), including signal detrending, rhythmicity assessment before and after the treatment time, construction of PTCs, and statistical testing using bootstrapping methods. For PTC analysis cells were selected by being trackable for the entire experiment, by goodness of fit of a cosine function ($R^2 > 0.5$), and by their period length (between 22 and 29 h).

Specifically for analysis of reporter amplitude (Supplementary Fig. 5B, C), the following procedure was performed: for each cell, the signal was detrended by normalizing to a 24-h moving average trend (instead of z-score normalization), and the difference between the max and mean intensities of the detrended signal in $t = [24, 96]$ was taken as the amplitude of that cell.

Rat serum was obtained in conformity with the Weizmann Institute Animal Care and Use Committee guidelines and kindly provided by Avigdor Schertz's lab.

PTC statistical evaluation

PTC statistical analysis was performed as previously described¹². Briefly, the raw PTC data were fitted with two Fourier models for either type 1 or type 0 resetting. To test whether any phase response is present in a certain group, we bootstrapped from control (untreated) group samples in the size of the test group 1000 times. In each iteration, a Fourier model was fitted, and the maximal shift was retrieved. The null hypothesis (namely, no phase shift) was rejected if the resampled maximal shift was higher than the observed maximal shift less than 5% of the times. To select between type 1 and type 0 models, the root-mean-square deviation (RMSE) was calculated for each fit as a measure of goodness-of-fit (i.e., should be minimized for an optimal fit). We bootstrapped from the tested group 1000 times. In each

iteration, both models were fitted to the resampled data, and RMSE was calculated for them. The type 1 RMSE should be larger than the type 0 RMSE 90% of the time to reject the null hypothesis of type 1 resetting.

Resampling of period distribution

To match the distributions of two populations, we implemented a selective resampling approach in MATLAB. Our method randomly samples from the target "before" period distribution and then looks for the closest value in the source distribution. The data sampled from the source is then used to reconstruct a PTC in the standard procedure described above.

RNA extraction and quantitative PCR

RNA was extracted at day 9.5 post-seeding, from 6-well tissue culture plates, by a standard TRI-reagent (Sigma) RNA extraction protocol. RNA concentration was determined using NanoDropTM 2000 Spectrophotometer (Thermo Fisher Scientific). Synthesis of cDNA was performed using qScript cDNA SuperMix (Quanta Biosciences).

Real-time PCR assays were performed using SYBR green with LightCycler II machine (Roche) and normalized to the geometrical mean of three housekeeping genes: *Hprt*, *Rplp0*, *Tbp*. All primers used in this study were previously reported in refs. 13,39, except for *Dec1* and *Npas2*, which were designed using Primer3 software 4.1.0 (default settings) and validated by generating a calibration curve. Primer sequences are listed in Supplementary Table 1.

siRNA transfections

Cells were seeded at densities of 0.25×10^5 or 2×10^5 cells per well in 24-well or 6-well plates, respectively, using DMEM (Gibco) supplemented with 10% FBS (Gibco), 11 mM glutamine (Biological Industries), 100 U/mL penicillin, and 100 mg/mL streptomycin (Biological Industries) (PSG). The day after seeding, cells were transfected with 25 nM siRNA and 5 μ l of Lipofectamine RNAiMax (ThermoFisher) transfection reagent as per the manufacturer's protocol. Post-transfection, the media was replaced the next day with FluoroBrite DMEM (Gibco) supplemented with 1% FBS and 1% PSG (see scheme in Fig. 3a), and cells were analyzed according to the circaSCOPE protocol.

For clock gene expression analysis, 48 h post media replacement, cells were exposed to 2% rat serum for 0, 3, and 6 h, RNA was extracted, and expression levels of the different clock genes were analyzed by quantitative PCR (see Supplementary Table 1 for list of primers).

Co-immunoprecipitation assay

HEK293 cells were transfected with either pCDNA3-FLAG (empty vector) or pCDNA3-FLAG-mCRY2 using JetPEI (Polyplus) following the manufacturer's protocol. Dexamethasone (4 nM) was added 24 h post-transfection for 16 h. Cells were harvested and protein extracts were prepared using NP-40 lysis buffer (50 mM HEPES pH 7.4, 150 mM NaCl, 1 mM MgCl₂, 1% NP-40) supplemented with protease inhibitors cocktail (1:100, MERCK MILLIPORE, 539134), phosphatase inhibitor cocktail 3 (1:100, Sigma, P0044), and DTT (1:2000). FLAG-CRY2 was immunoprecipitated using anti-FLAG M2-affinity gel beads (Sigma, A2220). Proteins were separated by SDS-PAGE, transferred to nitrocellulose membrane, and analysed by immunoblotting using the following antibodies: anti-GR (Cell Signaling, D6H2L), anti-FLAG (Sigma, F3165), and anti-TUBULIN (Sigma, T9026).

Phase resetting of wild type and *Cry2* knockout *Bmal1*-luciferase reporter U2OS cells

We employed wild type and *Cry2* knockout *Bmal1*-luciferase reporter U2OS cells²³. 5×10^5 cells were seeded in 3-cm culture dish using DMEM (Gibco) supplemented with 10% FBS (Gibco), 11 mM glutamine (Biological Industries), 100 U/mL penicillin, and 100 mg/mL streptomycin (Biological Industries) (PSG). The following day, the medium was

replaced with phenol red-free DMEM (Gibco) supplemented with 1% FBS, 1% PSG, and 100 nM D-Luciferin (Promega). After the medium change, the cells were transferred to a LumiCycle32 incubated luminometer (Actimetrics), where bioluminescence was continuously recorded and treated with dexamethasone 63 h post media change.

GRE bioluminescence reporter assay

For real-time GRE bioluminescence measurements, NIH-3T3 cells were seeded in 3-cm plates (100,000 cells per plate). One day post-seeding, cells were transfected with 1 µg of GRE-Luc plasmid (a kind gift from Yosef Yarden⁴⁰), alongside siNT or siCry2 using JetPRIME transfection reagent (Polyplus). The day after transfection, the medium was replaced with phenol red-free DMEM supplemented with 1% FBS, 1% PSG, and 100 nM D-luciferin. The cells were then transferred to a LumiCycle32 incubated luminometer. Cells were treated with 4 nM dexamethasone after about 60 h from recording start, and evaluated for induction 24 h post treatment.

Chemical compounds

All inhibitors used in Fig. 1 and Supplementary Fig. 1 were sourced from the TargetMol brand at 100 nM. The labels of the compounds are specified in the respective figures, and these inhibitors were ordered as working samples from the Weizmann Drug Discovery Unit. Dexamethasone and progesterone were purchased from Sigma.

Statistics and software availability

Statistical analyses and data visualization were performed using MATLAB (R2024b, MathWorks).

Reporting summary

Further information on research design is available in the Nature Portfolio Reporting Summary linked to this article.

Data availability

All the data from this study are included in the article, supporting information and the Supplementary Data 1–9. Source data are provided with this paper.

Code availability

The CellProfiler custom pipeline and the MATLAB code for post-analysis are available through GitHub (<https://doi.org/10.5281/zenodo.5139820>)⁴¹.

References

1. Bolshette, N., Ibrahim, H., Reinke, H. & Asher, G. Circadian regulation of liver function: from molecular mechanisms to disease pathophysiology. *Nat. Rev. Gastroenterol. Hepatol.* **20**, 695–707 (2023).
2. Patke, A., Young, M. W. & Axelrod, S. Molecular mechanisms and physiological importance of circadian rhythms. *Nat. Rev. Mol. Cell Biol.* **21**, 67–84 (2020).
3. Reinke, H. & Asher, G. Crosstalk between metabolism and circadian clocks. *Nat. Rev. Mol. Cell Biol.* **20**, 227–241 (2019).
4. Sulli, G., Manoogian, E. N. C., Taub, P. R. & Panda, S. Training the circadian clock, clocking the drugs, and drugging the clock to prevent, manage, and treat chronic diseases. *Trends Pharm. Sci.* **39**, 812–827 (2018).
5. Mohawk, J. A., Green, C. B. & Takahashi, J. S. Central and peripheral circadian clocks in mammals. *Annu. Rev. Neurosci.* **35**, 445–462 (2012).
6. Takahashi, J. S. Transcriptional architecture of the mammalian circadian clock. *Nat. Rev. Genet.* **18**, 164–179 (2017).
7. Adamovich, Y., Ladeuix, B., Golik, M., Koenders, M. P. & Asher, G. Rhythmic oxygen levels reset circadian clocks through HIF1alpha. *Cell Metab.* **25**, 93–101 (2017).
8. Balsalobre, A. et al. Resetting of circadian time in peripheral tissues by glucocorticoid signaling. *Science* **289**, 2344–2347 (2000).
9. Gerber, A. et al. Blood-borne circadian signal stimulates daily oscillations in actin dynamics and SRF activity. *Cell* **152**, 492–503 (2013).
10. Hirota, T. & Fukada, Y. Resetting mechanism of central and peripheral circadian clocks in mammals. *Zool. Sci.* **21**, 359–368 (2004).
11. Johnson, C. H. Phase response curves: What can they tell us about circadian clocks? In *Circadian Clocks from Cell to Human*, (eds. Hiroshige, T. & Honma, K.-i.), 209–249 (Sapporo, Hokkaido University Press, 1992).
12. Manella, G., Aizik, D., Aviram, R., Golik, M. & Asher, G. Circa-SCOPE: high-throughput live single-cell imaging method for analysis of circadian clock resetting. *Nat. Commun.* **12**, 5903 (2021).
13. Manella, G., Bolshette, N., Golik, M. & Asher, G. Input integration by the circadian clock exhibits nonadditivity and fold-change detection. *Proc. Natl. Acad. Sci. USA* **119**, e2209933119 (2022).
14. Balsalobre, A., Marcacci, L. & Schibler, U. Multiple signaling pathways elicit circadian gene expression in cultured Rat-1 fibroblasts. *Curr. Biol.* **10**, 1291–1294 (2000).
15. Manella, G. et al. The human blood transcriptome exhibits time-of-day-dependent response to hypoxia: lessons from the highest city in the world. *Cell Rep.* **40**, 111213 (2022).
16. Bourgeois, S., Pfahl, M. & Baulieu, E. E. DNA binding properties of glucocorticosteroid receptors bound to the steroid antagonist RU-486. *EMBO J.* **3**, 751–755 (1984).
17. Balsalobre, A., Damiola, F. & Schibler, U. A serum shock induces circadian gene expression in mammalian tissue culture cells. *Cell* **93**, 929–937 (1998).
18. Shigeyoshi, Y. et al. Light-induced resetting of a mammalian circadian clock is associated with rapid induction of the mPer1 transcript. *Cell* **91**, 1043–1053 (1997).
19. Ramanathan, C. et al. Cell type-specific functions of period genes revealed by novel adipocyte and hepatocyte circadian clock models. *PLoS Genet.* **10**, e1004244 (2014).
20. Webb, A. B., Taylor, S. R., Thoroughman, K. A., Doyle, F. J. 3rd & Herzog, E. D. Weakly circadian cells improve resynchrony. *PLoS Comput. Biol.* **8**, e1002787 (2012).
21. Kawano, T., Inokuchi, J., Eto, M., Murata, M. & Kang, J. H. Activators and inhibitors of protein kinase C (PKC): their applications in clinical trials. *Pharmaceutics* **13**, 1748 (2021).
22. Moughal, N., Stevens, P. A., Kong, D., Pyne, S. & Pyne, N. J. Adenylate cyclase, cyclic AMP and extracellular-signal-regulated kinase-2 in airway smooth muscle: modulation by protein kinase C and growth serum. *Biochem. J.* **306**, 723–726 (1995).
23. Bording, T., Abdo, A. N., Maier, B., Gabriel, C. & Kramer, A. Generation of human CRY1 and CRY2 knockout cells using duplex CRISPR/Cas9 technology. *Front. Physiol.* **10**, 577 (2019).
24. Lamia, K. A. et al. Cryptochromes mediate rhythmic repression of the glucocorticoid receptor. *Nature* **480**, 552–556 (2011).
25. Roenneberg, T. & Merrow, M. The circadian clock and human health. *Curr. Biol.* **26**, R432–R443 (2016).
26. Burchett, J. B., Knudsen-Clark, A. M. & Altman, B. J. MYC ran up the clock: the complex interplay between MYC and the molecular circadian clock in cancer. *Int. J. Mol. Sci.* **22**, 7761 (2021).
27. Tischkau, S. A. Mechanisms of circadian clock interactions with aryl hydrocarbon receptor signalling. *Eur. J. Neurosci.* **51**, 379–395 (2020).
28. Kon, N. et al. CaMKII is essential for the cellular clock and coupling between morning and evening behavioral rhythms. *Genes Dev.* **28**, 1101–1110 (2014).
29. Zagni, C. et al. PTEN mediates activation of core clock protein BMAL1 and accumulation of epidermal stem cells. *Stem Cell Rep.* **9**, 304–314 (2017).

30. Karatsoreos, I. N., Wang, A., Sasanian, J. & Silver, R. A role for androgens in regulating circadian behavior and the suprachiasmatic nucleus. *Endocrinology* **148**, 5487–5495 (2007).
31. Lamia, K. A. et al. AMPK regulates the circadian clock by cryptochrome phosphorylation and degradation. *Science* **326**, 437–440 (2009).
32. Manella, G. et al. Hypoxia induces a time- and tissue-specific response that elicits intertissue circadian clock misalignment. *Proc. Natl. Acad. Sci. USA* **117**, 779–786 (2020).
33. Shao, S., Zhao, H., Lu, Z., Lei, X. & Zhang, Y. Circadian rhythms within the female HPG axis: from physiology to etiology. *Endocrinology* **162**, bqab117 (2021).
34. DeMayo, F. J., Zhao, B., Takamoto, N. & Tsai, S. Y. Mechanisms of action of estrogen and progesterone. *Ann. N. Y. Acad. Sci.* **955**, 48–59 (2002).
35. Masuda, K., Yoshimoto, R., Li, R., Sakurai, T. & Hirano, A. Parameterized resetting model captures dose-dependent entrainment of the mouse circadian clock. *Nat. Commun.* **16**, 1421 (2025).
36. Masuda, K. et al. Singularity response reveals entrainment properties in mammalian circadian clock. *Nat. Commun.* **14**, 2819 (2023).
37. Del Olmo, M. et al. Are circadian amplitudes and periods correlated? A new twist in the story. *F1000Res* **12**, 1077 (2023).
38. Carpenter, A. E. et al. CellProfiler: image analysis software for identifying and quantifying cell phenotypes. *Genome Biol.* **7**, R100 (2006).
39. Cho, H. et al. Regulation of circadian behaviour and metabolism by REV-ERB-alpha and REV-ERB-beta. *Nature* **485**, 123–127 (2012).
40. Srivastava, S. et al. ETS proteins bind with glucocorticoid receptors: relevance for treatment of Ewing sarcoma. *Cell Rep.* **29**, 104–117.e104 (2019).
41. Manella, G. Circa-SCOPE (v0.2). <https://doi.org/10.5281/zenodo.5139820> (2021).

Acknowledgements

We are grateful to all the members of the Asher lab for their comments on the manuscript. We wish to thank Reinat Nevo, Ehud Sivan and Ofra Golani for their advice on the image analysis pipeline (Life Science Core Facilities, Weizmann Institute of Science). We thank Haim Barr (head of the Drug Discovery Unit of the Weizmann Institute of Science) for the inhibitors used in our screen. G.A. is supported by the European Research Council (ERC-2022-PoC CircaSCOPE101060296), Minerva Stiftung, Bina, Dr. Barry Sherman Institute for Medicinal Chemistry, Abisch Frenkel Foundation for the Promotion of Life Sciences, Adelis Foundation, Susan and Michael Stern. G.M. is supported by the Human Frontiers Science Program (LT0037/2023-L) and is an alumnus of the Zuckerman Israeli Postdoc Program.

Author contributions

Conceptualization: S.E., G.M., and G.A.; Investigation: S.E., G.M., N.B., M.G., and Y.A.; Visualization: S.E. and G.M.; Data Curation: S.E. and G.M.; Reagents: A.K.; Software: G.M.; Funding: G.A.; Writing–Review & Editing: S.E., G.M., and G.A.

Competing interests

The authors declare no competing interests.

Additional information

Supplementary information The online version contains supplementary material available at <https://doi.org/10.1038/s41467-025-67349-5>.

Correspondence and requests for materials should be addressed to Gad Asher.

Peer review information *Nature Communications* thanks Eric Zhang and the other anonymous reviewer(s) for their contribution to the peer review of this work. A peer review file is available.

Reprints and permissions information is available at <http://www.nature.com/reprints>

Publisher's note Springer Nature remains neutral with regard to jurisdictional claims in published maps and institutional affiliations.

Open Access This article is licensed under a Creative Commons Attribution-NonCommercial-NoDerivatives 4.0 International License, which permits any non-commercial use, sharing, distribution and reproduction in any medium or format, as long as you give appropriate credit to the original author(s) and the source, provide a link to the Creative Commons licence, and indicate if you modified the licensed material. You do not have permission under this licence to share adapted material derived from this article or parts of it. The images or other third party material in this article are included in the article's Creative Commons licence, unless indicated otherwise in a credit line to the material. If material is not included in the article's Creative Commons licence and your intended use is not permitted by statutory regulation or exceeds the permitted use, you will need to obtain permission directly from the copyright holder. To view a copy of this licence, visit <http://creativecommons.org/licenses/by-nc-nd/4.0/>.

© The Author(s) 2025